Reprinted from
INTERNATIONAL JOURNAL OF COMPUTER AND INFORMATION SCIENCES

Vol. 14, No. 3, June 19
Printed in Belgiu

Finding Minimal Enclosing Boxes

Joseph O'Rourke[1]

Received July 1984; revised April 1985

The problem of finding minimal volume boxes circumscribing a given set three-dimensional points is investigated. It is shown that it is not necessary for minimum volume box to have any sides flush with a face of the convex hull the set of points, which makes a naive search problematic. Nevertheless, it proven that at least two adjacent box sides are flush with edges of the hull, ar this characterization enables an $O(n^3)$ algorithm to find all minimal boxes for set of n points.

KEY WORDS: Computational geometry; polyhedra; polyhedral approx mation; minimum volume box.

1. INTRODUCTION

It is often useful to circumscribe a complex three-dimensional shape with simpler shape, for, e.g., intersection calculations; other applications incluc layout,[1] image processing,[2] and shape analysis.[3] The proble investigated in this paper is, given a set of n points in three dimensio (which may be the vertices of a polyhedron), find the minimum volum rectangular boxes circumscribing the points. The boxes may be oriente arbitrarily, but all faces must meet orthogonally. Henceforth such box will be called *minimal boxes*. Note that there is not necessarily a uniqu minimum: for example, an icosahedron has 30 distinct equal-volume minima.[2]

The equivalent problem in two-dimensions is to find minimal area re tangles circumscribing n points in a plane. This problem has been solve with an $O(n)$ algorithm by Toussaint,[4] based on earlier work by Freema

[1] Department of Electrical Engineering and Computer Science, Johns Hopkins Universi Baltimore, Maryland 21218.

[2] Each of 10 pairs of parallel faces admits 3 identical but combinatorially distinct minimu volume boxes.

0091-7036/85/0600-0183$04.50/0

and Shapira.[1] Algorithms for minimal area triangles[5,6] and minimal area k-gons,[7] have also been developed.

There are two simplifications that can be made to the problem immediately. First, it is obvious that every box circumscribing a set of n points also circumscribes the convex hull of those points. Since the convex hull of a set of n three-dimensional points can be found in $O(n \log n)$ time,[8] and since this time will be dominated in our algorithm by the remaining computations, our first step is to compute the convex hull of the given points. We will assume henceforth that the input is a convex polyhedron of n vertices.

Second, it is obvious that a minimal box must touch the inscribed polyhedron on each of its six faces; otherwise a face could be moved inwards reducing the volume.

2. TWO EDGES FLUSH

In this section we will supplement the two obvious necessary conditions just discussed with one less obvious: every minimal box must have at least two adjacent faces flush with edges of the enclosed polyhedron. First we will review the results in two dimensions.

Define an side s of a circumscribing rectangle to be *flush* with an edge e of the inscribed polygon if $e \subseteq s$. Freeman and Shapira[1] proved the following theorem.

Theorem 1. A minimal area rectangle circumscribing a convex polygon has at least one side flush with an edge of the polygon.

Toussaint[4] was able to use this characterization to implement a "rotating calipers" algorithm to find all minimal rectangles in linear time. The algorithm fixes a rectangle side flush to an arbitrary polygon edge, then finds the other contact points as extreme points of the polygon in directions orthogonal and parallel to the fixed side. The area of this initial rectangle is computed. The "next" candidate is found by determining, from the clockwise angles at each contact, which of the contacts will change first as the rectangle rotates clockwise. Its area is compared to the minimal so far, and the procedure repeated. Theorem 1 guarantees that this procedure will find all minima.

Define a face F of a circumscribing box to be *flush* with an edge e of the inscribed polyhedron if $e \subseteq F$. The analog to Theorem 1 for three dimensions is as follows.

Theorem 2. A box of minimal volume circumscribing a convex

polyhedron must have at least two adjacent faces flush with edges of the polyhedron.

Proof. Suppose to the contrary that there are fewer that two adjacent faces flush with edges. We will show that there must be four adjacent faces, all orthogonal to one (forming a ring), that are not flush with any edges. Let the faces be called *Front*, *Back*, *Left*, *Right*, *Bottom* and *Top*.

Case 1. Exactly one face, say *Bottom*, is flush with an edge. Then *Front*, *Left*, *Back*, *Right* form the claimed ring.

Case 2. Exactly two nonadjacent faces are flush with an edge. Let one be *Bottom*. Then only *Top* is nonadjacent to *Bottom*, so the other face flush with an edge must be *Top*. Then again *Front*, *Left*, *Back*, *Right* form the claimed ring.

Case 3. More than two faces are flush with edges. Since each face is adjacent to four others, it is not possible to select more than two faces such that none are adjacent to each other.

Without loss of generality, let *Front*, *Left*, *Back*, *Right* be the ring of nonflush faces. Project the polyhedron and the ring of faces onto the *Bottom* face. The result is a convex polygon circumscribed by a rectangle. Since none of the faces are flush with an edge of the polyhedron, none of the rectangle edges are flush with an edge of the projected convex polygon. Theorem 1 then says that the rectangle is not minimal in area. We can therefore decrease the volume of the supposed minimal box by keeping *Bottom* and *Top* fixed and rotating the other faces until their projected rectangle becomes flush with an edge of the projected polygon. This contradiction establishes the theorem. ∎

I do not believe that Theorem 2 can be strengthened. For example, it is easy to establish that it is not necessary for any face of a minimal box to be flush with a *face* of the inscribed polyhedron: the minimal box for a regular tetrahedron has all six faces flush with edges, but none flush with faces (see Fig. 1).

Our algorithm checks all pairs of edges as candidates for the flush edges guaranteed by the theorem, and for each pair performs a type of three-dimensional caliper rotation. The data structure used to track the caliper rotation is discussed in the next section.

3. GAUSSIAN SPHERE REPRESENTATION

We will find it convenient to use a dual representation for a convex polyhedron P that we call the *Gaussian sphere* associated with P. The

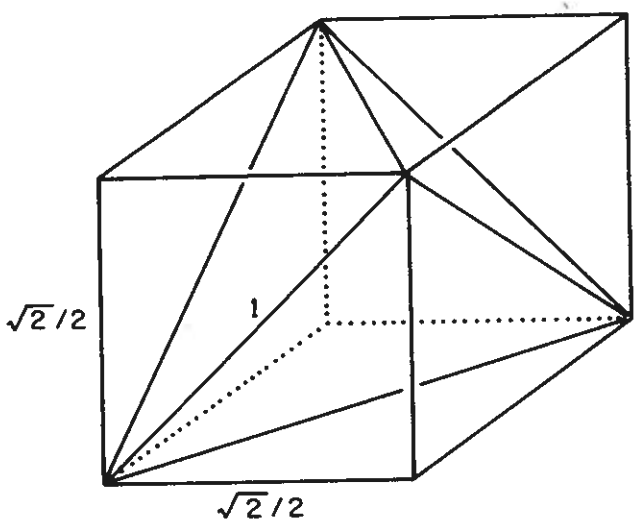

Fig. 1. The minimal box for a regular tetrahedron of edge length 1.

Gaussian sphere S partitions the surface of the unit sphere centered on the origin into convex regions $R(v)$, one for each vertex v of P, such that if $\mathbf{n}$ is a unit vector from the origin whose tip lies in $R(v)$, then the plane through v with normal $\mathbf{n}$ is a supporting plane for the polyhedron. Thus each vertex of P is associated with a region of S representing normals for all supporting planes at the vertex. Similarly, each face of P is mapped to a vertex of S representing its normal. And each edge of P is mapped to a subarc of a great circle on S, representing the normals of all supporting planes that contain the edge. Figure 2b shows the Gaussian sphere for the convex polyhedron in Fig. 2a.

It is easy to compute the Gaussian sphere representation in linear time from a data structure for a convex polyhedron that includes face and edge adjacency information, such as results from the Preparata and Hong convex hull algorithm[8]: simply create a vertex of S for each face of P, and an arc between two S vertices if the corresponding faces of P are adjacent.

It should be clear that each region R of S is convex in the sense that the shortest path on the surface of S (a great circle arc) between any two points of R is contained within R: every pair of supporting planes H_1 and H_2 at a vertex v of P intersect in a supporting line L at v such that all planes through L between H_1 and H_2 are also supporting, and L maps to a great circle arc connecting the images of H_1 and H_2 on S.

Any box surrounding a polyhedron P can be represented as three pairs of antipodal points on the Gaussian sphere, the tips of six orthogonal vectors emanating from the origin.[3] We will use S in the succeeding sections to track the "caliper paths," the locations where the box faces contact P, as the box moves from one orientation to the next.

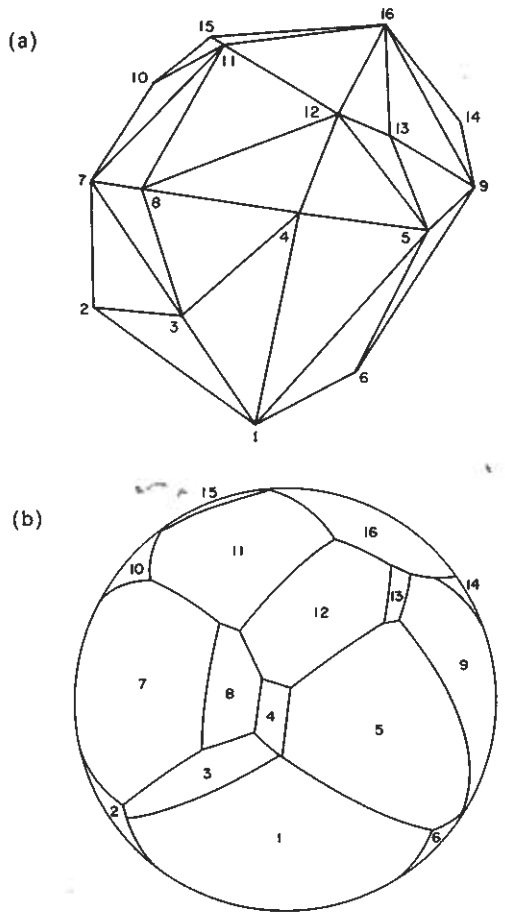

Fig. 2. (a) A convex polyhedron with 15 visible vertices. (b) The Gaussian sphere for the polyhedron. Each face is labeled with its corresponding vertex.

4. CALIPER PATHS

In this section we will establish that fixing two edges flush on adjacent faces leaves just a single degree of freedom. This will permit all the local

[3] Compare Toussaint's "star" data structure for the two-dimensional equivalent.[9]

minima that occur throughout the range of this freedom to be found in linear time. The constraints imposed by the two flush edges are a bit difficult to visualize, and it will be necessary to explore them in considerable algebraic detail. The reader interested in just the main line of thought may skip to Lemma 3 at the end of this section.

Let e_1 and e_2 be edges flush with the adjacent faces F_1 and F_2 (say *Left* and *Front*). Translate e_1 and e_2 to the origin O of a coordinate system as shown in Fig. 3. It is clearly no loss of generality to assume that e_1 coincides with the z-axis, and that e_2 lies in the yz-plane making an angle $\varphi \in [-\pi/2, \pi/2]$ with the y-axis; any other orientation may be rotated to such a configuration. We will also assume that e_1 and e_2 are unit vectors to simplify the calculations:

$$e_1 = (0, 0, 1) \tag{1}$$

$$e_2 = (0, \cos\varphi, \sin\varphi) \tag{2}$$

Let n_1 and n_2 be unit outward-pointing vectors normal to F_1 and F_2. The constraint that these faces are flush with e_1 and e_2 can be expressed as

$$n_1 \cdot e_1 = 0 \tag{3}$$

$$n_2 \cdot e_2 = 0 \tag{4}$$

Thus if n_1 and n_2 are placed at the origin O, n_1 must lie in the xy-plane, and n_2 must lie in a plane orthogonal to e_2; see Fig. 3. Let ϑ_1 be the angle

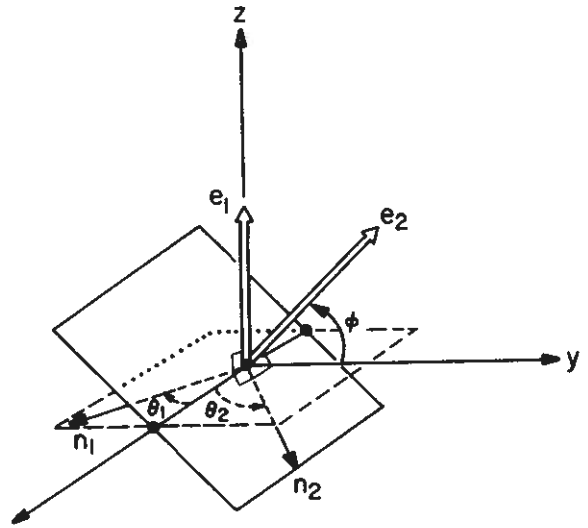

Fig. 3. n_1 is orthogonal to e_1, at angle ϑ_1 in the xy plane. n_2 is orthogonal to e_2, at angle ϑ_2 in the plane orthogonal to e_2.

from the positive x-axis to n_1; our conventions restrict ϑ_1 to lie in $[-\pi, 0]$. We have then

$$n_1 = (\cos\vartheta_1, \sin\vartheta_1, 0) \tag{5}$$

We now compute n_2 given φ, which fixes e_2, and ϑ_1, which fixes n_1. Let

$$n_2 = (x_2, y_2, z_2) \quad \text{with} \quad z_2 = \pm\sqrt{1 - x_2^2 - y_2^2} \tag{6}$$

We have two constraints on n_2: Eq. 4 and the orthogonality of F_1 and F_2:

$$n_1 \cdot n_2 = 0 \tag{7}$$

Solving Eqs. 4 and 7 simultaneously yields the following expressions for the components of n_2:

$$\begin{aligned} x_2 &= [-\sigma(\sin\varphi)] \sin\vartheta_1 \sin\varphi / R \\ y_2 &= [+\sigma(\sin\varphi)] \cos\vartheta_1 \sin\varphi / R \\ z_2 &= -\cos\vartheta_1 \cos\varphi / R \end{aligned} \tag{8}$$

where

$$R = \sqrt{\cos^2\vartheta_1 + \sin^2\vartheta_1 \sin^2\varphi} \tag{9}$$

and where $\sigma(x)$ is the sign function: $+1$ if $x \geq 0$ and -1 otherwise. These equations initially contain a pair of $\pm$'s, potentially leading to four solutions. But back substitution and our conventions show that the solution is unique for all ϑ_1, as shown in the previous equations.

Let ϑ_2 be the angle between the positive x-axis and n_2 (within the plane orthogonal to e_2): $\cos\vartheta_2 = x_2$, $\vartheta_2 \in [-\pi/2, \pi/2]$. Then we have established that, for a given e_1 and e_2, an orientation of F_1 flush with e_1 (specified by ϑ_1) uniquely determines an orientation of F_2 (specified by ϑ_2). Figure 4 plots the $(\vartheta_1, \vartheta_2)$ correspondence function for various values of φ. Note that when $\varphi = \pm\pi/2$, e_1 and e_2 are parallel and $\vartheta_2 = \pm(\vartheta_1 + \pi/2)$.

When $\varphi = 0$ and $\vartheta_1 = -\pi/2$, $R = 0$ and Eq. 8 are degenerate. Thus when e_1 and e_2 are orthogonal, ϑ_1 cannot move, but ϑ_2 is free to vary in $[-\pi/2, \pi/2]$, yielding solutions $n_2 = (\cos\vartheta_2, 0, \sin\vartheta_2)$.[4] We will see later that this degenerate simple motion is a special case of the general motion, and does not have to be considered separately.

[4] In addition the roles of e_1 and e_2 are symmetrical, so ϑ_1 and ϑ_2 can be interchanged.

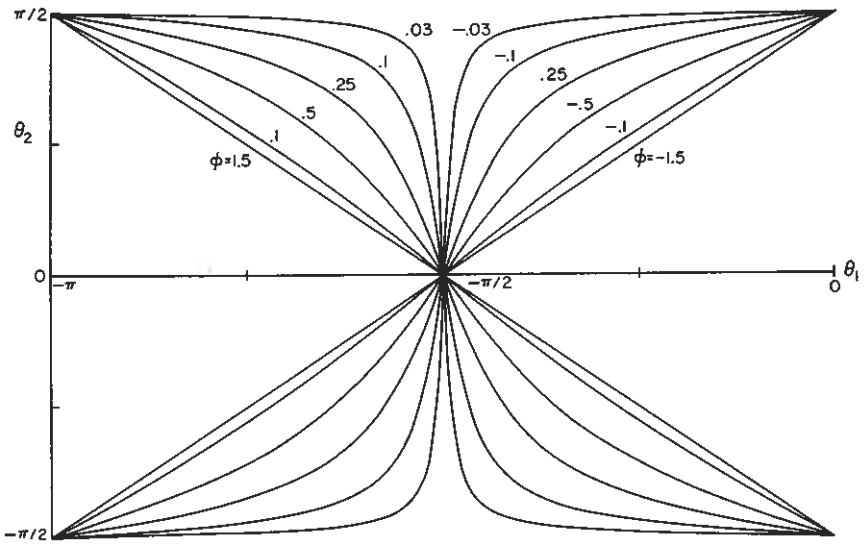

Fig. 4. ϑ_2 as a function of ϑ_1 for various values of φ.

Finally we explore the behavior of $n_3 = (x_3, y_3, z_3)$, the outward-pointing normal for the *Top* face of the box. The defining equation

$$n_3 = n_1 \times n_2 \tag{10}$$

leads, after simplification, to

$$\begin{aligned} x_3 &= z_2 \sin \vartheta_1 \\ y_3 &= -z_2 \cos \vartheta_1 \\ z_3 &= -x_2/\sin \vartheta_1 \end{aligned} \tag{11}$$

Figure 5 plots (x_3, y_3) as ϑ_1 and ϑ_2 are varied throughout their ranges. The (x_3, y_3) image is a convex shape through the origin, symmetric about the y-axis. Thus as ϑ_1 and ϑ_2 vary, n_3 precesses about a cone shape in three dimensions. This somewhat counter-intuitive twisting motion of the box is displayed for a particular φ value in Fig. 6. When e_1 and e_2 are parallel, n_3 remains fixed as ϑ_1 and ϑ_2 vary. Note that this is the same motion induced by the degenerate solution when e_1 and e_2 are orthogonal, except that in that case n_1 remains fixed as the other two normals rotate.

We can summarize the calculations of this section in the following lemma.

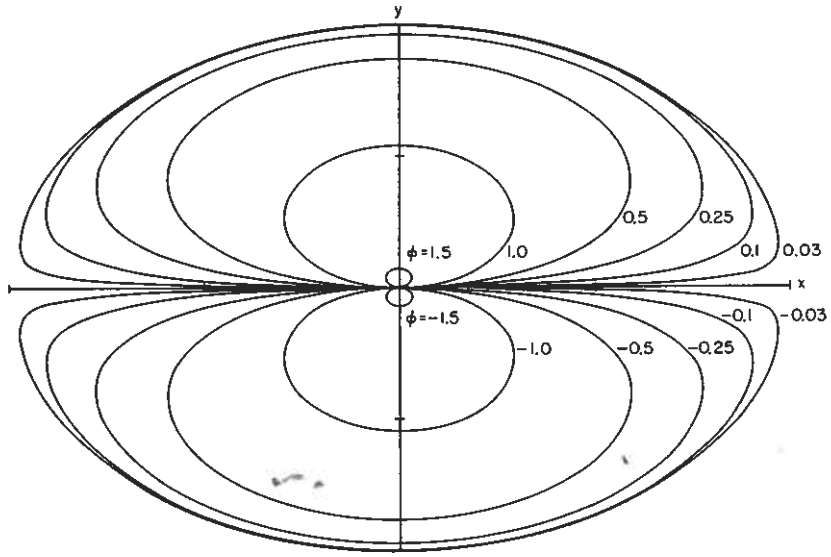

Fig. 5. The trace of n_3, seen from above, as ϑ_1 and ϑ_2 vary, for selected values of φ.

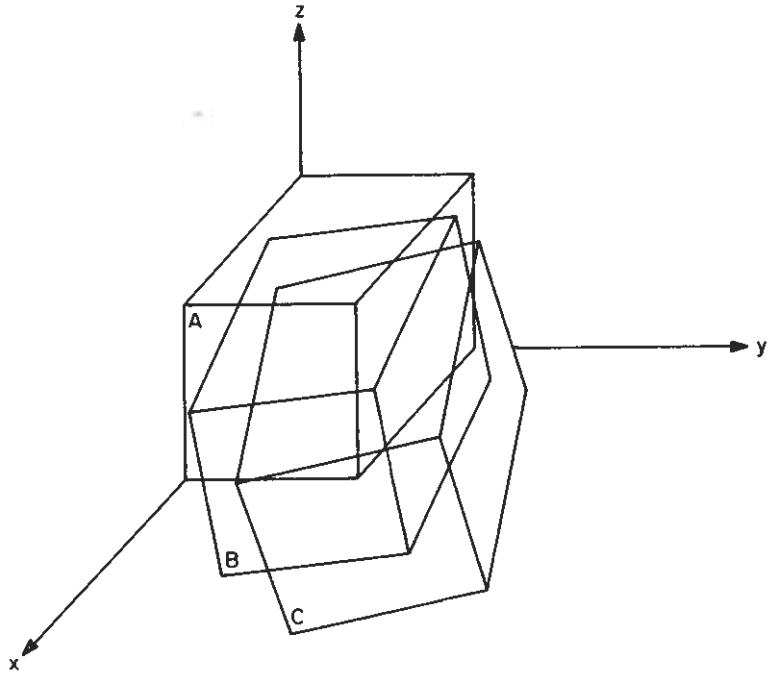

Fig. 6. Three orientations of a box for $\vartheta_1 = -\pi/2(A)$, $-1.4(B)$, $-1.2(C)$; here $\varphi = 0.5$.

Lemma 3. Let n_1 and n_2 be normals to two adjacent faces flush with edges of the polyhedron, and let n_3 be orthogonal to both n_1 and n_2. Then n_1 uniquely determines n_2 and n_3 via easily calculable relations (Eqs. 8 and 11). As n_1 is moved throughout its free range, both n_1 and n_2 trace out arcs of great circles on the Gaussian sphere, and n_3 traces out a curved convex path.

Proof. The unique determination is established by the referenced equations. The normals n_1 and n_2 trace out the edges on S corresponding to e_1 and e_2, which are great circle arcs, as discussed in Section 3. Thus their antipodal partners are also great circle arcs. That the n_3 path is convex is obvious from Fig. 5, and will be formally established in the next section. ∎

5. THE ALGORITHM

The algorithm is reminiscent of Toussaint's two-dimensional "rotating calipers" at the local level,[4] but is a brute-force search at the top level. The algorithm tries all pairs of edges as candidates for the two flush edges guaranteed by Theorem 2. At the top level the algorithm is as follows.

Construct Gaussian sphere for the given convex polyhedron.

for all pairs of edges e_1 and e_2 *do*
  Rotate 3 orthogonal "calipers" throughout ϑ_1 range,
  computing volume of each local minimum.
return global minima

Constructing the Gaussian sphere requires $O(n)$ time as shown in Section 3; its use will be discussed later in this section. The *for* loop executes

$$\binom{n}{2} = O(n^2)$$

times. We will now show how the body of the loop can be implemented with an $O(n)$ algorithm.

Start ϑ_1 at its smallest possible value (when F_1 is flush with one of the two faces adjacent to e_1), or with the smallest value permitted by the range of freedom of ϑ_2, which is easily computed from the equations in the previous section. Fixing ϑ_1 fixes all three normals by Lemma 3. Now find the contact for each of the remaining four faces by finding the extremes in the appropriate directions. These extremes can be found in $O(\log n)$ time,[10] but we can settle for a linear search. This establishes the starting position for the "calipers."

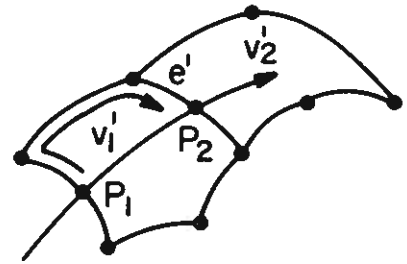

Fig. 7. Contact change occurs when the normal tip enters or leaves a face, here at p_1 and p_2.

Now the goal is to compute the next value of ϑ_1 at which at least one of the four contacts is different. This is accomplished by looking at the normal tip paths on the Gaussian sphere. A contact change occurs whenever a path crosses an edge separating two regions (see Fig. 7). Let unprimed variables refer to vertices, edges, and faces of the polyhedron P, and primed variables to their counterparts on S. As the path crosses from region v_1' over e' to region v_2' on S, the supporting plane determined by the normal changes its contact from vertex v_1, to edge e briefly, then to vertex v_2 on P. So we must find the "next" such crossing among all four paths.

Consider first the paths for $-n_1$ and $-n_2$, determining faces F_3 and F_4. Since these are great circle arcs, they can intersect a convex region v' of S at most twice, say at p_1 and p_2 as in Fig. 7. Then, given p_1, we can search for p_2 by traversing the edges of v' counterclockwise until the great circle is met again. Knowing p_1 and p_2 either directly yields a $\Delta\vartheta_1$ (for an n_1 path), or indirectly (for n_2) via the equations in the preceding section.

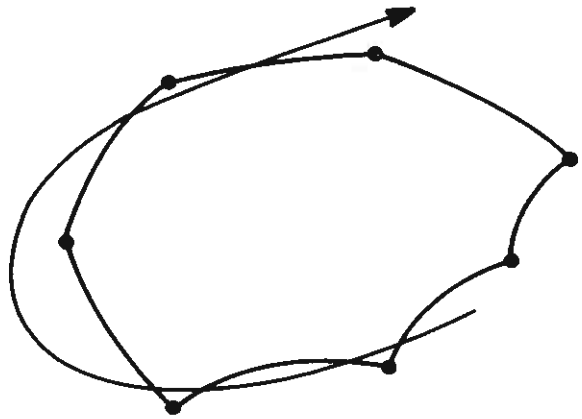

Fig. 8. The n_3 path intersections with a face are sorted on the boundary of the face.

The paths for the two faces orthogonal to n_3, F_5 and F_6, are not great circle arcs, and therefore may intersect a region at several places. However, as such a path is convex, its intersections with v' are sorted cyclically around the boundary of v', as in Fig. 8. We can establish this formally by showing that an n_3 path intersects each great circle at most twice.

Let (x, y, z) be a normal vector whose tip lies on a great circle. Then, if (a, b, c) is a normal orthogonal to the plane of the great circle, we have

$$ax + by + cz = 0 \tag{12}$$

Substituting Eq. 11 for x, y, and z and simplifying yields a second degree trigonometric polynomial:

$$a' \cos \vartheta_1 \sin \vartheta_1 + b' \cos^2 \vartheta_1 + c' \sin^2 \vartheta_1 = 0 \tag{13}$$

where a', b', and c' are independent of ϑ_1. Such an equation can have at most two roots within any range of π for ϑ_1. This can be seen by replacing $\cos \vartheta_1 \sin \vartheta_1$ with $\frac{1}{2}\sin 2\vartheta_1$, and $\cos^2 \vartheta_1$ and $\sin^2 \vartheta_1$ with $\frac{1}{2}(1 \pm \cos 2\vartheta_1)$, yielding a first-degree trigonometric equation in $2\vartheta_1$. This equation can have at most one root within a π range of $2\vartheta_1$, and so at most 2 roots within a π range of ϑ_1, establishing the claim.

Since the intersections of an n_3 path with a region of S are sorted cyclically, we can still find the next intersection via a counterclockwise search of the region's boundary. Determining whether a particular edge of the region intersects the path requires solving Eq. 13, which can be accomplished in constant time by standard numerical techniques. This immediately yields a $\Delta\vartheta_1$ value.

Among all four paths, the one yielding the smallest $\Delta\vartheta_1$ determines the next combinatorial position of the calipers. Between these two positions, no contacts change. We will show in the next section that we can find the minimal volume box within the $\Delta\vartheta_1$ range in constant time. Given this, it is easy to see that the search of the entire ϑ_1 range requires only $O(n)$ time: each path intersects each edge on the Gaussian sphere at most twice, so the entire computation is bounded by the number of edges on the sphere, which is $O(n)$.

We can summarize this discussion with the following algorithm for performing the caliper rotation.

$\vartheta_1 \leftarrow$ minimum possible value
while $\vartheta_1 <$ maximum possible value *do*
begin
  Find the next intersection of the $-n_1$, $-n_2$, and $\pm n_3$ paths with an edge on S.
  $\Delta\vartheta_1 \leftarrow$ smallest $\Delta\vartheta_1$ determined by the four paths.
  Find the minimum volume box withing the range $[\vartheta_1, \vartheta_1 + \Delta\vartheta_1]$.
  $\vartheta_1 \leftarrow \vartheta_1 + \Delta\vartheta_1$.
end

6. THE VOLUME FUNCTION

The equations developed in Section 4 enable us to formulate an explicit expression for the volume within any $\Delta\vartheta_1$ range during which the contacts do not change. It can be expressed as a function of one variable, ϑ_1, and is a trigonometric polynomial of fixed degree. Somewhat surprisingly, we will show that this function can have positive local minima, implying that volume local minima may occur with just two flush edges, and all four other faces with vertex contacts. The reader uninterested in the algebraic details may skip to the summarizing lemma at the end of this section.

Consider viewing the box from the positive z axis, looking directly down e_1. Let the contact on F_3 (directly opposite F_1) have a projection as shown in Fig. 9: it is at a distance c_1 in the xy-plane, and oriented such that when $\vartheta_1 = \gamma_1$, the thickness of the box in that dimension is maximal. In general the thickness is given by

$$d_1 = c_1 \cos(\vartheta_1 - \gamma_1) \tag{14}$$

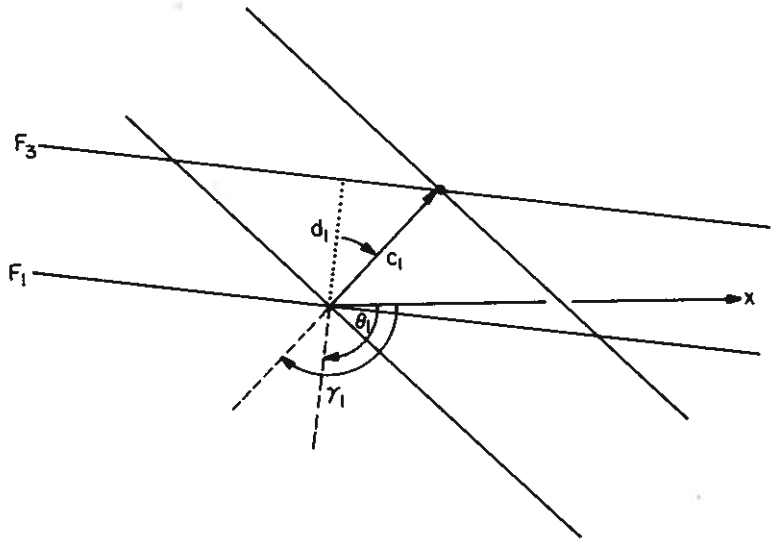

Fig. 9. Top view of thickness: maximum is achieved at $\vartheta_1 = \gamma_1$.

Note that when $d_1 < 0$, face F_1 has rotated beyond the F_3 contact point, a physically impossible situation.

Similarly, we can specify the thickness in the second dimension with an angle γ_2 at which ϑ_2 rotation about e_2 achieves the maximal thickness c_2:

$$d_1 = c_2 \cos(\vartheta_2 - \gamma_2) \tag{15}$$

The thickness in the third dimension is a bit more complicated, since neither F_5 nor F_6 is rotating about an edge; rather both are (in general) pivoting on vertices as ϑ_1 moves throughout an interval. Let c_3 be a vector between the two contact points. Then the thickness is determined by the angle this vector makes with the third normal:

$$d_3 = c_3 \cdot n_3 \tag{16}$$

As we are only interested in the variation of the volume as a function of ϑ_1, not its absolute magnitude, we will normalize so that $c_1 = c_2 = 1$ and c_3 is a unit vector.

Each of these three equations may be written as functions of ϑ_1 by using the relationships established in Section 4. The result is:

$$\begin{aligned} d_1 &= \cos\vartheta_1(\cos\gamma_1) + \sin\vartheta_1(\sin\gamma_1) \\ d_2 &= [\cos\vartheta_1(\sin\gamma_2) + \sin\vartheta_1(\cos\gamma_2 \sin\varphi)]/R \\ d_3 &= [\cos\vartheta_1 \sin\vartheta_1(a\cos\varphi) + \cos^2\vartheta_1(-b\cos\varphi) + (-c\sin\varphi)]/R \end{aligned} \tag{17}$$

where, in the final equation, $c_3 = (a, b, c)$. Multiplying these three equations yields an equation for the volume V as a function of ϑ_1. Three typical plots of V versus ϑ_1 are shown in Fig. 10. Note that curves B and C have no positive local minima. This implies that the minimum volume box is achieved by pushing ϑ_1 forward or backwards as far as is permitted while continuing to maintain the same contacts; in other words, the minimum is achieved at a contact transition point. But curve A demonstrates that the function can have a positive local minimum for certain arrangements of contacts. Thus not all minima are achieved at extreme positions: a delicate balancing might be required.

The volume function has the form

$$V = \frac{P_4(\cos\vartheta_1, \sin\vartheta_1)}{P_2(\cos\vartheta_1, \sin\vartheta_1)} \tag{18}$$

where P_4 is a 4th degree polynomial in $\cos\vartheta_1$ and $\sin\vartheta_1$, and $P_2 = R^2$ (Eq. 9) is a second degree polynomial. Thus the equation $dV/d\vartheta_1 = 0$ is a

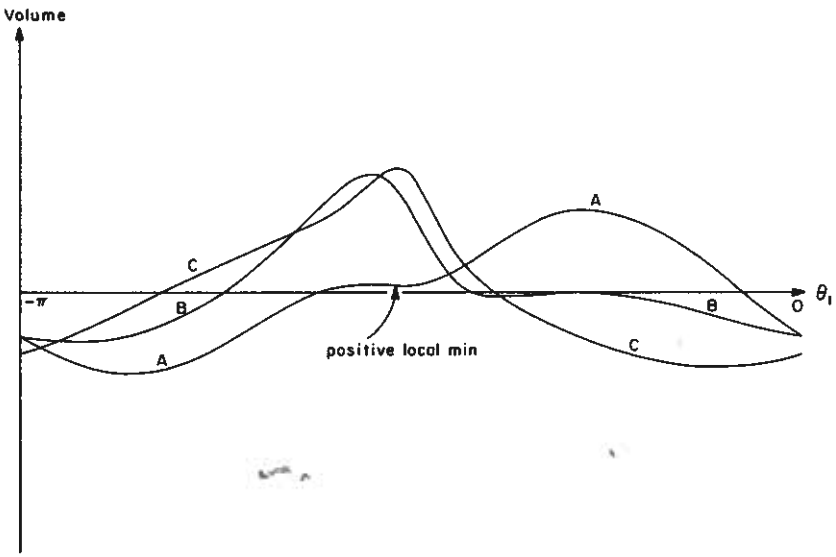

Fig. 10. Three plots of the volume function. A: $(\varphi, \gamma_1, \gamma_2, c_3) = (.5, -1.8, -.9, (0, .99, .05))$; B: $(-.3, -2.4, -.4, (.4, .77, .5))$; C: $(.2, -1, .5, (0, .8, .6))$.

6th degree polynomial in $\cos\vartheta_1$ and $\sin\vartheta_1$ (after multiplying out the denominator). This equation has at most 6 roots within the π range of ϑ_1, implying that there are at most 3 local volume minima within this range. Some of these minima may fall in the regions where the volume is negative, indicating an impossible situation. In fact, I have not been able to find an example that has more than one positive local minimum. In any case, the volume is a smooth, well-behaved function, and it is easy to find the minima by standard numerical techniques. For example, the roots of the derivative could be found by converting the 6th degree trigonometric equation to a 12th degree polynomial in u by substituting $\cos\vartheta_1 = u$ and $\sin\vartheta_1 = \sqrt{1-u^2}$ and squaring, and then finding the roots of this polynomial by any root extraction method. The simplicity of the function, however, suggests that a more straightforward numerical search for minima would be sufficient.

The theoretical import of this section is summarized in the following lemma.

Lemma 4. The volume, when expressed as a function of ϑ_1, has at most 3 local minima, whose locations are given by roots of a 6th degree trigonometric polynomial. Thus the minimum volume within any range of ϑ_1 may be found in constant time.

7. DISCUSSION

The "delicate balancing" that might be required for achieving a minimum volume box is not too surprising, as such balancing is required even for the minimum area triangle in two dimensions. But in the case of the triangle, the balancing condition has a concise geometrical interpretation: it was proven in Ref. 5 by a geometrical argument that the balancing edge must pivot on its midpoint. This same result was arrived at independently in Ref. 11 by minimizing the area function.[11] In this latter algebraic formulation, the midpoint characterization is not immediately obvious from the equations. It may be, similarly, that there is a concise geometric interpretation of the volume function minima that is masked by the increased complexity of the three-dimensional equations.

It should also be noted that although we have established that local minima may require balancing, no example has been constructed that has a globally minimal box balanced on four point contacts.

Although the described algorithm requires $O(n^3)$ time to find all minima, no example is known that has more than $\Omega(n)$ global minima. A cylinder with regular n-gons as end caps has $n/4$ equal global minima, establishing the $\Omega(n)$ lower bound. Adding a vertex just above the center of each end cap of this example creates a polyhedron that has $\Omega(n^2)$ local minima, but it still has only a linear number of global minima. The gap between the lower bound and the algorithm's complexity indicates that it may not be optimal.

Finally, the complicated calculations required by the presented algorithm lead one to consider approximation algorithms. A simple $O(n^2)$ algorithm will find all minimal boxes with at least one box side flush with a *face* of the polyhedron. For each face F of the $O(n)$ faces of the polyhedron, fix one box side, say *Bottom*, flush to F, determining the opposite side *Top* as extreme in the orthogonal direction. Now project the polyhedron onto the *Bottom* box side, and solve the two-dimensional minimal area rectangle problem by Toussaint's algorithm in $O(n)$ time.[4] The convex hull of the projection can be found in linear time by only projecting those edges of the polyhedron whose adjacent face normals point both towards and away from *Bottom*. Thus when iterated over all faces, the algorithm requires $O(n^2)$ time. Applying this algorithm to a regular tetrahedron of unit edge length yields a box of volume $1 \cdot \sqrt{3}/2 \cdot \sqrt{2/3} = 1/\sqrt{2}$; the true minimum (Fig. 1) has half this volume: $(\sqrt{2}/2)^3 = 1/(2\sqrt{2})$.

ACKNOWLEDGMENTS

I thank Robert St. Amant for preparing the computer-drawn figures, and Michael McKenna for the tetrahedron example and several other useful comments.

REFERENCES

1. H. Freeman and R. Shapira, Determining the Minimum-area Encasing Rectangle for an Arbitrary Closed Curve, *Commun. of the ACM*, **18**:409–413 (July 1975).
2. F. C. A. Groen, P. W. Verbeek, N. de Jong, and J. W. Klumper, The Smallest Box Around a Package, *Pattern Recognition*, **14**(1–6):173–178 (1981).
3. K. R. Sloan, Jr., Analysis of "Dot Product Space" Shape Descriptions, *IEEE Trans. on Pattern Analysis and Machine Intelligence*, **PAMI-4**(1):87–90 (January 1982).
4. G. T. Toussaint, Solving Geometric Problems with the "Rotating Calipers," *Proc. of IEEE MELECON 83*, Athens, Greece (May 1983).
5. V. Klee and M. L. Laskowski, Finding the Smallest Triangles Containing a Given Convex Polygon, *J. Algorithms*, **6**:457–464 (1985).
6. J. O'Rourke, A. Aggarwal, S. Maddila, and M. Baldwin, An Optimal Algorithm for Finding Minimal Enclosing Triangles, *J. Algorithms*, to appear (1986).
7. J. S. Chang and C. K. Yap, A Polynomial Solution for Potato-peeling and Other Polygon Inclusion and Enclosure Problems, *Proc. of Foundations of Comput. Sci.*, pp. 408–416 (October 1984).
8. F. P. Preparata and S. J. Hong, Convex Hulls of Finite Sets of Points in Two and Three Dimensions, *Commun. of the ACM*, **20**:87–93 (October 1977).
9. G. T. Toussaint, Pattern Recognition and Geometric Complexity, *Proc. 5th Inter. Conf. on Pattern Recognition*, Miami Beach, p. 1324–1347 (December 1980).
10. H. Edelsbrunner and H. Mauer, Finding Extreme Points in Three Dimensions and Solving the Post-office Problem in the Plane, *Info. Proc. Letters*, **21**:39–47 (1985).
11. D. Dori and M. Ben-Bassat, Circumscribing a Convex Polygon by a Polygon of Fewer Sides with Minimal Area Addition, Comp. Vision, Graphics, and Image Processing, **24**:131–159 (1983).

Printed by the St. Catherine Press Ltd., Tempelhof 41, Bruges, Belgium